Artificial Intelligence in Medicine (2007) 41, 237–250

ELSEVIER

ARTIFICIAL INTELLIGENCE IN MEDICINE

http://www.intl.elsevierhealth.com/journals/aiim

Multiscale analysis of short term heart beat interval, arterial blood pressure, and instantaneous lung volume time series

Leonardo Angelini [a,b,c], Roberto Maestri [d], Daniele Marinazzo [a,b,c,*], Luigi Nitti [a,c,e], Mario Pellicoro [a,b,c], Gian Domenico Pinna [d], Sebastiano Stramaglia [a,b,c], Salvatore A. Tupputi [b]

[a] *TIRES-Center of Innovative Technologies for Signal Detection and Processing, University of Bari, Via Amendola 173, 70126 Bari, Italy*
[b] *Dipartimento Interateneo di Fisica, Via Amendola 173, 70126 Bari, Italy*
[c] *Istituto Nazionale di Fisica Nucleare, Sezione di Bari, Via Amendola 173, 70126 Bari, Italy*
[d] *Dipartimento di Bioingegneria, Fondazione Salvatore Maugeri, IRCCS, Istituto Scientifico di Montescano, 27040 Montescano, Pavia, Italy*
[e] *Dipartimento di Biochimica Medica, Biologia Medica e Fisica Medica, University of Bari, Piazza G.Cesare, 70125 Bari, Italy*

Received 30 January 2007; received in revised form 11 July 2007; accepted 12 July 2007

KEYWORDS
Multiscale entropy analysis;
Autoregressive models;
Physiological time series

Summary

Motivations: Physiological systems are ruled by mechanisms operating across multiple temporal scales. A recently proposed approach, multiscale entropy analysis, measures the complexity at different time scales and has been successfully applied to long term electrocardiographic recordings. The purpose of this work is to show the applicability of this methodology, rooted on statistical physics ideas, to short term time series of simultaneously acquired samples of heart rate, blood pressure and lung volume, from healthy subjects and from subjects with chronic heart failure. In the same spirit, we also propose a multiscale approach, to evaluate interactions between time series, by performing a multivariate autoregressive (AR) modeling of the coarse grained time series.
Methods: We apply the multiscale entropy analysis to our data set of short term recordings. Concerning the multiscale version of the multivariate AR approach, we apply it to the four dimensional time series so as to detect scale dependent patterns of interactions between the physiological quantities.

* Corresponding author at: Dipartimento di Fisica, Universitá degli Studi di Bari, Campus Universitario, Via Amendola 173, 70126 Bari, Italy. Tel.: +39 0805442391; fax: +39 0805442434.
E-mail address: daniele.marinazzo@ba.infn.it (D. Marinazzo).

0933-3657/$ – see front matter
doi:10.1016/j.artmed.2007.07.012

Results: Evaluating the complexity of signals at the multiple time scales inherent in physiologic dynamics, we find new quantitative indicators which are statistically correlated with the pathology. Our results show that multiscale entropy calculated on all the measured quantities significantly differs ($P < 10^{-2}$ and less) in patients and control subjects, and confirms the *complexity-loss* theory of aging and disease. Also applying the multiscale autoregressive approach significant differences were found between controls and patients; in the sight of finding a possible diagnostic tools, satisfactory results came also from a receiver-operating-characteristic curve analysis (with some values above 0.8).
Conclusions: The multiscale entropy analysis can give useful information also when only short term physiological recordings are at disposal, thus enlarging the applicability of the methodology. Also the proposed multiscale version of the multivariate regressive analysis, applied to short term time series, can shed light on patterns of interactions between cardiorespiratory variables.

1. Introduction

Physiological systems are ruled by mechanisms operating across multiple temporal scales. Many approaches have been developed in the last years to analyze these complex signals, including, for example, studies of: Fourier spectra [1,2], chaotic dynamics [3,4], scaling properties [5,6], multifractal properties [7,8], correlation integrals [9], $1/f$ spectra [10,11], synchronization properties [12], and multivariate autoregressive (AR) methods [13,14]. A deep insight on the fundamental mechanisms of biological systems can be achieved by studying complexity, one of the key features of physiological time series. The underlying dynamics of such systems spans a great range of frequencies, therefore a complete analysis must include a multiple time-scale approach. A recently proposed approach, multiscale entropy (MSE) analysis [15], has been applied to heart rate dynamics [16], human gait [17] and neuronal behavior [18]. Furthermore, another measure aimed to calculate complexity at different time scales has been introduced in [19]. In [15], the degree of complexity of time series is compared at varying temporal scale, and MSE analysis is applied to 24 h electrocardiographic recordings of healthy subjects, subjects with congestive heart failure, and subjects with atrial fibrillation. Healthy and young dynamics are the most complex (see also [20—22]): these results support the general *complexity-loss* theory, according to which de-complexification of systems is a common feature of pathological conditions, as well as of aging; when physiologic systems become less complex, their information content is degraded. As a result, they are less adaptable and less able to cope with the exigencies of a constantly changing environment.

On the other hand, obtaining long time series may be difficult and expensive in some applications; a method working also on short time series (not longer than 10 min) would allow a larger applicability in those cases. In particular, use of short time series would allow the realization of devices able to record and process the signals in real time.

In this paper we show that MSE analysis may also be successfully applied to short term physiological recordings, still obtaining relevant information about the underlying mechanisms. In particular, we consider simultaneous recordings of electrocardiogram, respiration signal and arterial blood pressure, and discuss the ability to diagnose chronic heart failure (CHF), a disease associated with major abnormalities of autonomic cardiovascular control.

Besides entropy-based methods, interactions between time series have been widely studied with linear predictive models [13,14]. We thus implement the multiscale paradigm in this frame by considering a multiscale version of the classical multivariate AR analysis of time series, to find scale-dependent patterns of interactions between the physiological time series here considered.

In the next section we describe MSE and multiscale AR methods, and the short term physiological data here analyzed. In Section 3 the results obtained on our data set are reported. These findings are discussed in Section 4. Some conclusions are drawn in Section 5.

2. Methods and data

2.1. The multiscale entropy (MSE) analysis

We briefly recall the multiscale entropy (MSE) method [15]. Given a one-dimensional discrete time series, consecutive coarse grained time series, corresponding to scale factor τ, are constructed in the following way. First, the original time series is

divided into non-overlapping windows of length τ, where the length is defined in unit of samples; then, data points inside each window are averaged, so as to remove fluctuations with time scales smaller than τ. For scale one, the coarse grained time series is simply the original time series; the length of each coarse grained time series is equal to the length of the original time series divided by the scale factor τ. Finally an entropy measure S_E is calculated for each coarse grained time series and plotted as function of the scale factor τ. S_E coincides with the parameter $S_E(m,r)$, introduced by Pincus [23] and Richman and Moorman [24], see also [25], termed *sample entropy*, and given by

$$S_E(m,r) = -\ln\left(\frac{A}{B}\right). \quad (1)$$

For clarity's sake we recall here how A and B are defined. For a time series of N points, the vector $\mathbf{x}_m(i)$ is made of m consecutive recordings starting at index i, with i running from 1 to $N-m$; for each i, $B_i^r(m)$ is then defined as the number of vectors $\mathbf{x}_m(j)$ within r of $\mathbf{x}_m(i)$, for $i \neq j$, multiplied by $(N-m-1)^{-1}$. In the same way, $A_i^r(m)$ is defined as the number of vectors $\mathbf{x}_{m+1}(j)$ within r of $\mathbf{x}_{m+1}(i)$ ($i \neq j$), multiplied by $(N-m-1)^{-1}$. B is given by $[(N-m-1)/2]\sum_{i=1}^{N-m} B_i^r(m)$, and A is given by $[(N-m-1)/2]\sum_{i=1}^{N-m} A_i^r(m)$.

This sample entropy is related to the probability that sequences from the time series, which are close (within r) for m points, remain close at the subsequent data point. In the original proposal both the sequence length m and the tolerance parameter r were kept fixed as τ was varied, so that changes in S_E on each scale were depending both on the regularity and the variability of the coarse grained sequences [26,27]. In the present work we take r, at each τ, inversely proportional to the standard deviation (S.D.) of the coarse grained time series, and consider separately how the S.D. of signals varies with the time scale. As we show in Section 4, similar results are obtained applying the original prescription of Costa et al. [15]. Thus, as far as it concerns this application, it is not possible to state which methodology is the best.

Our goal is the processing of short time series; the dependence of sample entropy on the time series length has been already addressed in [28] with respect to white noise and $1/f$ noise. For $N=1000$ and white noise the discrepancy between the numerical and the mean value of S_E was found to be less than 1%, while being approximatively 12% in the case of $1/f$ noise. These findings suggest that stationarity is a fundamental requirement while dealing with short time series.

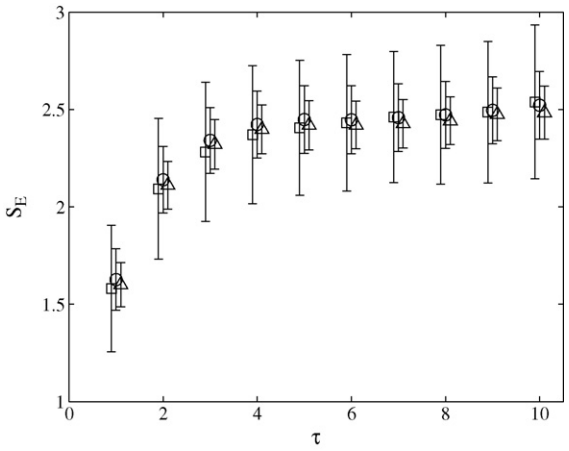

Figure 1 Multiscale entropy for rri time series of different lengths, extracted from Santa Fe data, vs. τ, averaged over 200 trials. Squares: length 1000 points; circles: length 5000 points; triangles: length 10,000 points. The values of τ for the three cases have been slightly shifted for better visualization.

Now we test the robustness of the proposed methodology on a benchmark problem from the Physionet data bank.[1]

We consider the recordings of lung volume (ilv) and R–R interval (rri) of a sleeping human suffering from sleep apnea, part of data set B of the Santa Fe Institute time series contest held in 1991. From the full time series, sampled at 2 Hz, we randomly extract segments of data with varying length ($N = 1000$, 5000 and 10,000 points) and evaluate the sample entropy for each realization. In Fig. 1, for the rri signal, we report S_E versus τ for the three values of N. The mean values are almost independent of N, whilst the standard deviation decreases as N increases. These results encourage applying the MSE approach on short term time series, as we will describe in the next section.

2.2. The multiscale AR analysis

We quantify the interactions between the time series at different time scales, in the frame of linear predictive models. To do so, we implement a multiscale version of AR modeling of time series. For each scale factor τ, we denote $\mathbf{x} = (\text{rri}, \text{sap}, \text{dap}, \text{ilv})$ the four-dimensional vector of the coarse grained time series of R–R interval (rri), systolic (sap) and diastolic (dap) blood pressure, and the instantaneous lung volume (ilv). At each scale, all coarse grained time series are normalized to have unit variance (see, e.g. [29]). A multivariate AR model of unity

[1] http://www.physionet.org (accessed 15 May 2007).

order is then fitted (by standard least squares minimization) to data:

$$\mathbf{x}(n) = C\,\mathbf{x}(n-1), \tag{2}$$

C is a 4×4 matrix, depending on τ, whose element C_{ij} measure the causal influence of jth time series on the ith one. Note that, unlike the typical AR modeling and in the spirit of the multiscale approach, here the order of the AR model is kept fixed and small: $m = 1$. Indeed information from longer and longer time scales is processed, in the AR fitting, as τ is increased, and the variations with τ of the elements of matrix C describe interactions between time series as a function of the scale.

We have applied the multiscale AR approach to the Physionet benchmark bivariate time series described in the previous subsection, on randomly extracted segments of data with varying length N. Matrix C is $2 \times 2n$ this case. Fig. 2 shows the plot of coefficient C_{12} (describing the action of ilv on rri) versus τ, and C_{21} (rri $\rightarrow$ ilv), for $N = 1000$, 5000 and 10,000. The interaction between these two time series has been already analyzed in [30], by means of the transfer entropy, and the strength rri $\rightarrow$ ilv was found to be slightly stronger than the reverse strength ilv $\rightarrow$ rri. The transfer entropy approach is a non-parametric method to evaluate interactions between time series, at a single scale, corresponding to $\tau = 1$; on the other hand the AR method is a linear and parametric method. Changing τ and applying the AR method on the resampled time series, one may look at different time scales. Now we describe our findings. We find that, at every τ, the influence of ilv on rri is negative, whilst the influence of rri on ilv is positive, see Fig. 2. At $\tau = 1$, the only value at which comparison with transfer entropy is possible, our results are consistent with those in [30]. For values of τ in the range [2,5] the modulus of C_{12} is higher and thus the interaction strength ilv $\rightarrow$ rri is dominant. This example shows that the multiscale AR modeling may put in evidence interdependencies, between time series, acting on different time scales.

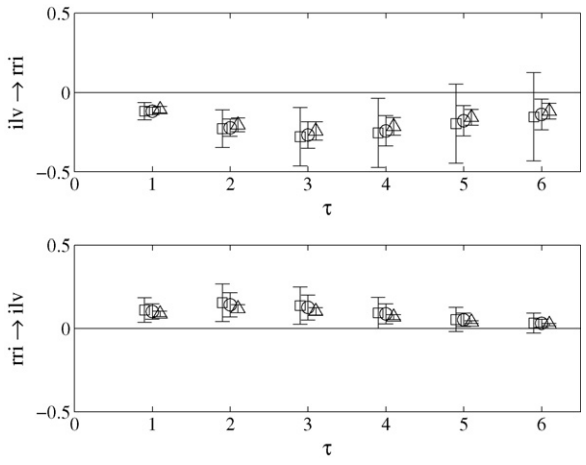

Figure 2 Causal relationships between heart rate and respiration from Santa Fe data set, averaged over 200 trials. Above: influence of respiration on heart rate; below: influence of heart rate on respiration. Squares: length 1000 points; circles: length 5000 points; triangles: length 10,000 points. The values of τ for the three cases have been slightly shifted for better visualization.

2.3. Data

Our data are from 47 healthy volunteers (age: 53 ± 8 years; M/F: 40/7) and 275 patients with chronic heart failure (CHF) (age: 52 ± 9 years; left ventricular ejection fraction: $28 \pm 8\%$; New York Heart Association class: 2.1 ± 0.7; M/F: 234/41), caused mainly by ischemic or idiopathic dilated cardiomyopathy (48% and 44%, respectively), consecutively referred to the Heart Failure Unit of the Scientific Institute of Montescano, S. Maugeri Foundation (Italy) for evaluation and treatment of advanced heart failure. Concerning the second group, cardiac death occurred in 54 (20%) of the patients during a 3-year follow-up. The cardiorespiratory data were collected both in conditions of spontaneous breathing (basal condition), and in regime of paced breathing [31,32]. Paced breathing is a simple experimental procedure that allows a better standardization in the measure of spectral indexes of cardiovascular variability (see for example [33] for a detailed in Section 4). After instrumentation and calibration were completed, the subjects, in supine position, carried out a session of familiarization with the paced breathing protocol. They were instructed to follow recorded instructions to breath in and out at a frequency of 0.25 Hz. After an initial trial, the subject were asked whether they felt comfortable with the paced breathing frequency, and an adjustment was made within $\pm 10\%$ of the target value. After signal stabilization, all the subjects were told to breath spontaneously, while they underwent a 10 min recording of ECG, lung volume (Respitrace Plus, Non-Invasive Monitoring Systems), and noninvasive arterial blood pressure (Finapres 2300, Ohmeda). The recordings were then repeated, again for 10 min, in the regime of paced breathing. R–R interval (resolution 1 ms), and systolic and diastolic arterial pressure values were obtained from the ECG and arterial pressure signals using custom made software [34]. The lung volume, R–R interval, systolic and diastolic pressure time series were resampled at a frequency of 2 Hz using a cubic spline interpolation. Part of this data set (the sap time series) has been already analyzed in [35] using a different approach.

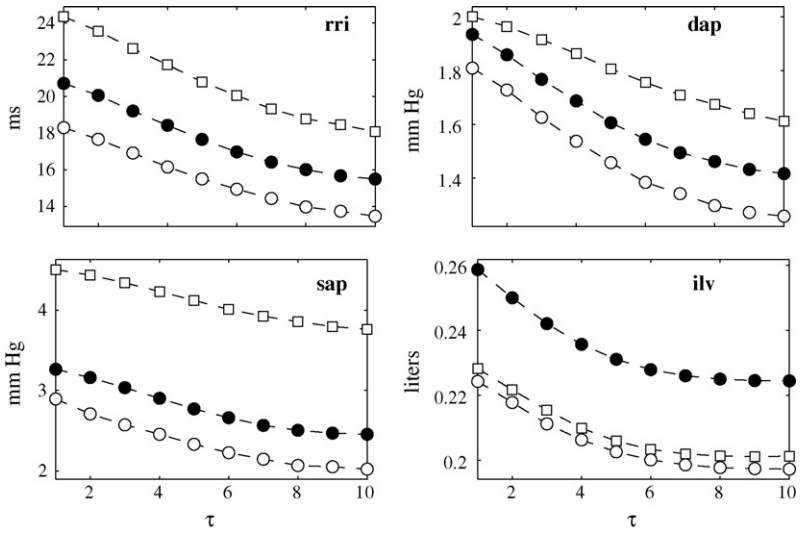

Figure 3 Standard deviations are plotted vs. τ for the coarse grained time series, in basal condition. Empty squares are the averages over the 47 healthy subjects, full circles are the averages over the 275 CHF patients, and empty circles are the averages over the 54 patients for whom cardiac death occurred. Top left: S.D. of rri time series. Top right: S.D. of dap time series. Bottom left: S.D. of sap time series. Bottom right: S.D. of ilv time series.

3. Results

Now we turn to the application to the data described in Section 2.3. In Fig. 3 we depict the standard deviations of the coarse grained time series in basal condition. Due to the short length of the samples at our disposal, we consider $\tau \leq 10$ so as to have sufficient statistics at each scale; this implies that our analysis will be limited to part of the high frequency (HF) band (0.15—0.45 Hz), the band in which the respiratory rhythm of most people lies. It is worth to stress that the use of paced breathing greatly reduces the spectral leakage of the respiratory components in other bands. In all cases, on average the standard deviation is a decreasing function of the scale; healthy subjects show greater variability than patients, except for ilv signals, where patients on average have the highest variability. Similar patterns of standard deviations are obtained in paced breathing conditions.

3.1. MSE results

As already stated, to extract the sample entropy from these signals, we take r equal to a fixed percentage (15%) of the standard deviations of the coarse grained time series; we take $m = 1$. We found this choice optimal for our short time series; however similar results were obtained using $m = 2$ as in [15]. In Fig. 4 we depict the average S_E of rri time series of controls, patients and dead patients, in basal condition (high) and paced breathing (low). On the right we depict, as a function of the scale factor τ, the probability that rri entropy values from controls and patients were drawn from the same distribution, evaluated by non-parametric Mann—Whitney test [36]: the discrimination is excellent at intermediate τ's. It is worth mentioning that here we compare subjects from the same age group, so that the decrease in heart rate variability cannot be accounted to age rather than disease. In the case of paced breathing the three curves get closer and the discrimination, between patients and controls, is decreased: thus paced breathing, in the case of rri entropy, reduces differences between patients and controls. We note that, on average, patients for whom cardiac death occurred show further reduced S_E with respect to the remaining CHF patients, thus suggesting that the complexity-loss paradigm also applies to the severity of the pathology.

In Fig. 5 we depict S_E of systolic arterial pressure (sap) time series. We find that at low τ patients have higher entropy, whilst at large τ they have lower entropy than controls. The crossover occurs at $\tau = 3$ in basal conditions, and $\tau \sim 6$ for paced breathing. The *complexity-loss* paradigm, hence, here holds only for large τ. This may be explained as an effect of respiration, whose influence becomes weaker as τ increases. This effect is more evident in conditions of paced breathing, due to synchronization [32,37]. Our results are consistent with those obtained in [35] using a different approach and with $\tau = 1$. It is interesting to observe that curves corresponding to dead patients are farther, from the controls curve, than the average curve from all patients, up to

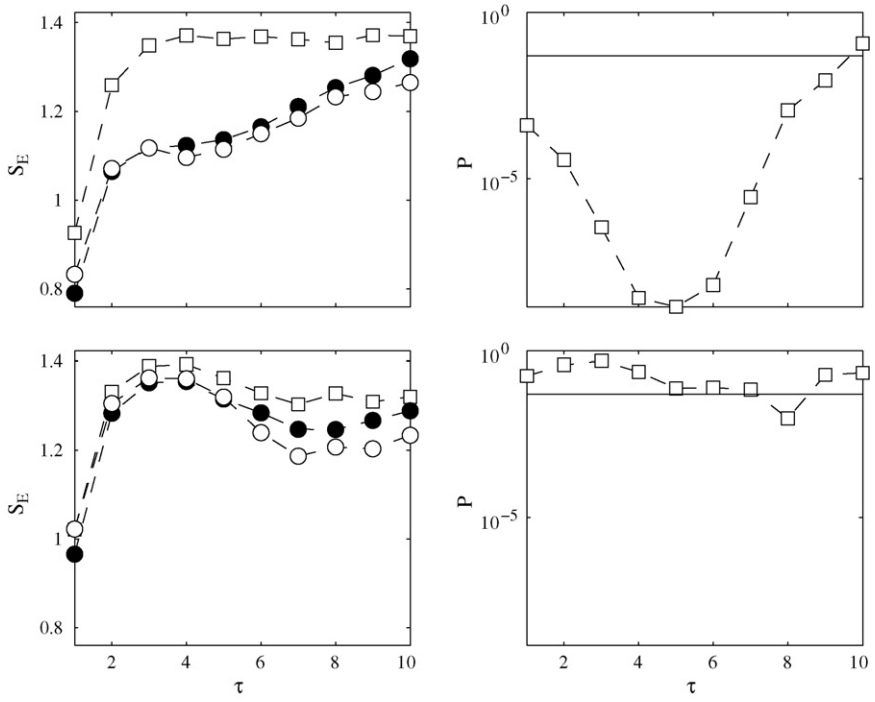

Figure 4 Sample entropy of rri time series plotted vs. τ. Empty squares are the averages over the 47 healthy subjects, full circles are the averages over the 275 CHF patients, and empty circles are the averages over the 54 patients for whom cardiac death occurred. Top left: S_E in basal condition. Top right: the probability that basal S_E values from controls and patients were drawn from the same distribution, evaluated by non-parametric test. Bottom left: S_E in paced breathing condition. Bottom right: the probability that paced breathing S_E values from controls and patients were drawn from the same distribution, evaluated by non-parametric test.

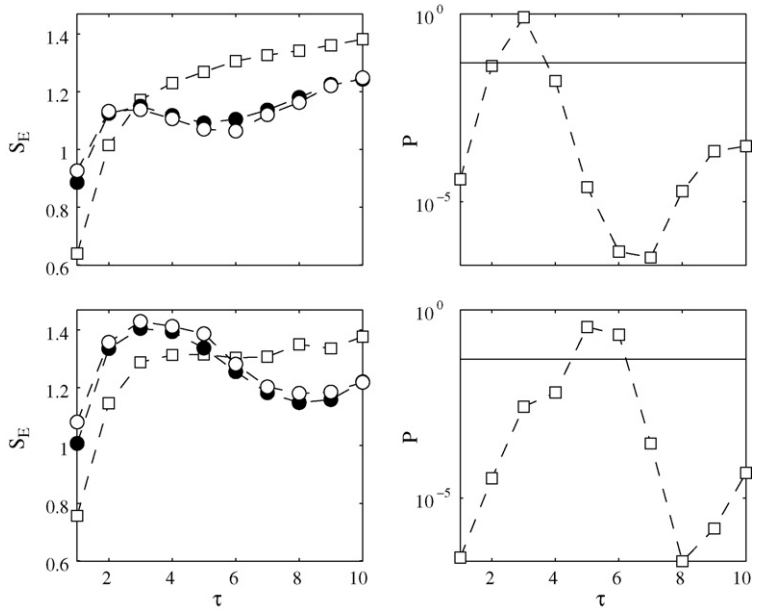

Figure 5 Sample entropy of sap time series plotted vs. τ. Empty squares are the averages over the 47 healthy subjects, full circles are the averages over the 275 CHF patients, and empty circles are the averages over the 54 patients for whom cardiac death occurred. Top left: S_E in basal condition. Top right: the probability that basal S_E values from controls and patients were drawn from the same distribution, evaluated by non-parametric test. Bottom left: S_E in paced breathing condition. Bottom right: the probability that paced breathing S_E values from controls and patients were drawn from the same distribution, evaluated by non-parametric test.

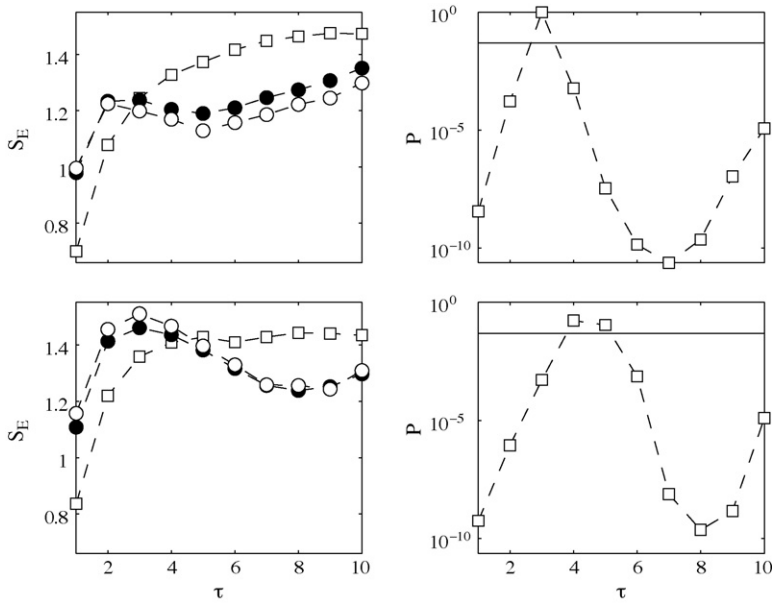

Figure 6 Sample entropy of dap time series plotted vs. τ. Empty squares are the averages over the 47 healthy subjects, full circles are the averages over the 275 CHF patients, and empty circles are the averages over the 54 patients for whom cardiac death occurred. Top left: S_E in basal condition. Top right: the probability that basal S_E values from controls and patients were drawn from the same distribution, evaluated by non-parametric test. Bottom left: S_E in paced breathing condition. Bottom right: the probability that paced breathing S_E values from controls and patients were drawn from the same distribution, evaluated by non-parametric test.

$\tau = 7$; departure from the controls curve appears to be connected with the severity of the disease.

In Fig. 6 we consider diastolic arterial pressure (dap) time series. We find a similar pattern to sap: patients have higher entropy at low τ and lower entropy than controls at large τ. Again the crossover occurs at $\tau = 3$ in basal conditions, and $\tau = 6$ for paced breathing.

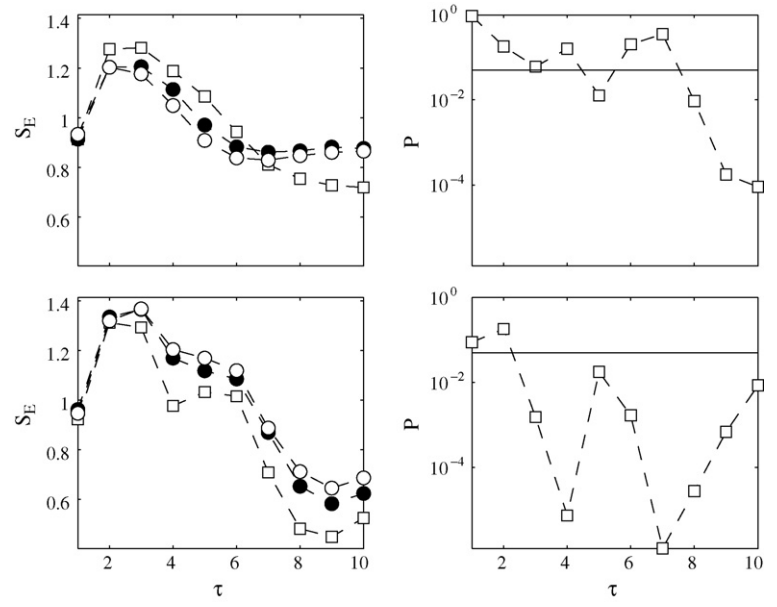

Figure 7 Sample entropy of ilv time series plotted vs. τ. Empty squares are the averages over the 47 healthy subjects, full circles are the averages over the 275 CHF patients, and empty circles are the averages over the 54 patients for whom cardiac death occurred. Top left: S_E in basal condition. Top right: the probability that basal S_E values from controls and patients were drawn from the same distribution, evaluated by non-parametric test. Bottom left: S_E in paced breathing condition. Bottom right: the probability that paced breathing S_E values from controls and patients were drawn from the same distribution, evaluated by non-parametric test.

Now we turn to consider ilv time series, as depicted in Fig. 7. In the basal case, controls have higher entropy at small scales. On the other hand controls show lower entropy than patients at $\tau > 7$: patients pathologically display fluctuations of ilv at larger scales than healthy subjects. Under paced breathing, controls are characterized by reduced fluctuations at high τ; at $\tau = 4$, when the window size is half of the respiration period, controls show a local minimum of the entropy. These phenomena are not observed for patients, where paced breathing is less effective in regularizing the ilv time series.

At this point, a comment is worth about the choice of parameters m and r for the calculation of sample entropy. The value of r determines the level of accepted noise; in the multiscale approach, m is kept fixed and small so that the influence of longer and longer time scales is probed as τ is increased. We verify that our results do not depend on the choice of m and r. Indeed, we find that as the value of r increases (m increases) the values of S_E, for both patients and controls, decrease. However the consistency of S_E values is preserved (see, e.g. Fig. 8, which refers to sap time series for paced breathing and $\tau = 1$: S_E is always greater for patients, independently of r and m). For a discussion of the optimal selection of m and r see [38].

In order to show now that the dynamics of the system is actually being measured, this analysis is applied to surrogate data, obtained by random shuffling of the temporal ordering of data samples. Fig. 9 reports the sample entropy for shuffled rri time series in paced breathing regime: it is clear that any structure and any discrimination between the three classes of subject is lost in this case.

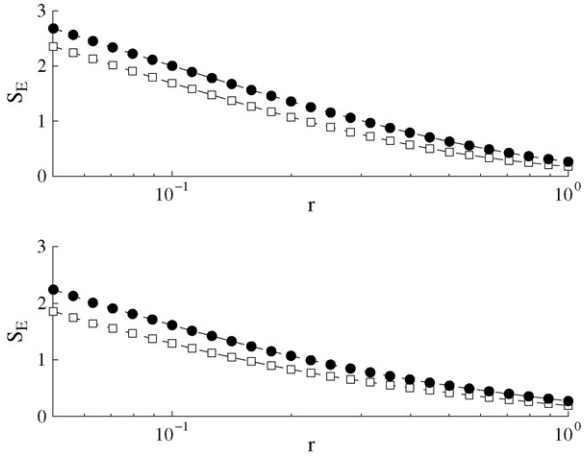

Figure 8 Sample entropy of sap time series plotted vs. r, in conditions of paced breathing and $\tau = 1$, for $m = 1$ (top) and $m = 2$ (bottom). Empty squares are the averages over the 47 healthy subjects, full circles are the averages over the 275 CHF patients.

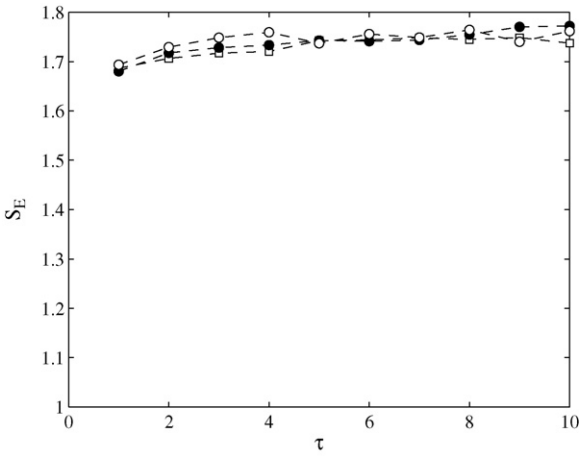

Figure 9 Sample entropy of shuffled rri time series in paced breathing regime plotted vs. τ. Empty squares are the averages over the 47 healthy subjects, full circles are the averages over the 275 CHF patients, and empty circles are the averages over the 54 patients for whom cardiac death occurred.

Similar results are obtained with the other quantities in both regimes.

The statistical separation between patients and controls, according to a given indicator, refers to the probability that its values are drawn from the same distribution. This definition is not connected with the diagnostic power of the indicator, which is to be quantified by other means. To evaluate the diagnostic power of the indicators above described, we measure the area under the receiver-operating-characteristic (ROC) curve [39], a well-established index of diagnostic accuracy; the maximum value of 1.0 corresponds to perfect assignment (unity sensitivity for all values of specificity) whereas a value of 0.5 arises from assignments to a class by pure chance. The results concerning the entropic indicators are reported in Table 1.

3.2. AR results

Coming to the AR analysis, in Table 2 we list the causal relationships which we find to be the most

Table 1 Area under ROC curve for MSE analysis

Series	τ	Area
rri, basal	5	0.7612
rri, paced breathing	8	0.6222
sap, basal	1	0.6884
sap, paced breathing	1	0.7388
dap, basal	1	0.7705
dap, paced breathing	1	0.7882
ilv, basal	9	0.6642
ilv, paced breathing	7	0.7258

Table 2 Causal relationships (averaged over controls, patients and dead patients)

Interaction	τ	Controls	Patients	Dead patients	*P*-value
rri → sap, basal	1	−0.0614	0.0128	0.0004	1.17×10^{-09}
rri → sap, paced breathing	1	−0.0721	0.0088	0.0076	5.76×10^{-11}
dap → rri, basal	1	0.0645	0.0092	0.0299	1.61×10^{-05}
	6	0.0787	−0.0552	−0.0665	5.54×10^{-09}
dap → rri, paced breathing	1	0.0981	0.0264	0.0321	5.63×10^{-05}
	6	0.1080	0.0121	0.0077	8.75×10^{-06}
rri → ilv, basal	4	0.0032	−0.0092	−0.0150	3.76×10^{-05}
rri → ilv, paced breathing	4	0.0129	−0.0101	−0.0049	2.09×10^{-05}
ilv → rri, basal	2	−0.2546	−0.2786	−0.2781	8.13×10^{-06}
rri → rri, basal	8	0.4430	0.6380	0.6680	6.50×10^{-09}
rri → rri, paced breathing	8	0.4470	0.5810	0.6120	8.22×10^{-04}
dap → dap, basal	1	0.9470	0.7500	0.7250	1.61×10^{-05}
dap → dap, paced breathing	1	0.9170	0.7380	0.7550	5.63×10^{-05}
sap → dap, basal	1	−0.0030	0.1070	0.1090	5.86×10^{-09}
sap → dap, paced breathing	1	0.0320	0.1470	0.1420	1.96×10^{-08}
	8	−0.2790	−0.0993	−0.1030	5.39×10^{-07}
ilv → sap, paced breathing	4	−0.2818	−0.2218	−0.1550	5.32×10^{-04}

discriminating between patients and the healthy subjects (controls). Firstly we consider the interactions between heart rate and blood pressure. In physiological conditions heart rate and arterial pressure are likely to affect each other as a consequence of the simultaneous feedback baroreflex regulation from sap−dap to rri and feedforward mechanical influence from rri to sap−dap [40].

For $\tau = 1$ the causal relationship rri → sap for controls is negative, both in basal and paced breathing conditions. Patients are characterized by weaker interaction, and at $\tau = 1$ the corresponding mean is positive. The difference between patient and controls is highly significant especially in paced breathing regime (*P*-value less than 10^{-10}). For dead patients the interaction is even weaker. The coefficient rri → dap shows a behavior very similar to those of rri → sap, i.e. it is negative and is stronger for controls.

The interaction dap → rri, as extracted by our approach, shows high discrimination between controls and patients both at low and high τ, see Table 1. In basal conditions, and for $\tau = 6$, this coefficient is positive for controls and negative for patients. Moreover, its strength is always smaller for patients with respect to controls.

Human respiration interacts with heart rate, originating the well known phenomenon of respiratory sinus arrhythmia [41,37,42]. We find that the interaction rri → ilv is significantly ($P < 10^{-4}$) stronger in controls than patients, under paced breathing and using $\tau = 4$. We also find that the interaction ilv → rri is negative and significantly ($P < 10^{-5}$) stronger in patients, in basal conditions and at high frequencies ($\tau \leq 4$).

Let us now turn to consider *self interactions* of time series. The matrix element A_{11} describes how much the rri signal depends on its value at the previous time. As it is shown in Table 1, both in basal and paced breathing conditions A_{11} is significantly lower for controls, especially at high τ. Also the self interaction of dap time series gives rise to an interesting pattern. It is stronger for controls, especially at low τ, leading to high discrimination between controls and patients at low τ.

The interaction of systolic and diastolic arterial pressure in healthy subjects has been recently studied in [43]. In the present analysis we find significant differences between patients and controls when the interaction sap → dap is considered, see Table 1. For controls, this coefficient is negative in basal conditions for $\tau = 1$, whereas it is positive and weaker in paced breathing regime, again for $\tau = 1$, becoming negative and stronger for $\tau = 8$.

It is known that respiration interacts in an open loop way with arterial pressure, mainly through a mechanical mechanism [44]. Our findings confirm it; indeed we find no significant sap → ilvinteraction, but significant ($P < 10^{-3}$) differences between patients and controls are found when the interaction ilv → sap is considered: controls show increased interaction w.r.t. patients.

Also for AR modeling we have applied the ROC analysis: for the two classes of controls and patients, in many cases we find fair discrimination (area between 0.7 and 0.8) or good discrimination

(between 0.8 and 0.9). The best ROC area is 0.874 and obtained using the values of dap → dap interaction at $\tau = 1$ and in basal conditions. Excellent (i.e., between 0.9 and 1) discrimination performances are obtained considering pairs of indicators and using Fisher linear discriminant (FLD) analysis to find the best linear combination of the two indicators; for example combining basal dap → dap interaction at $\tau = 1$ (alone provides 0.874 ROC area) and basal rri → sap interaction at $\tau = 1$ (alone provides 0.778 ROC area), leads to a FLD with 0.941 ROC area.

The separating performances in this case are poor. The indicators leading to the best ROC areas, as far as the discrimination between dead and alive patients is concerned, are dap → sap interaction in paced breathing conditions at $\tau = 1$ (0.622 ROC area) and dap sample entropy in paced breathing conditions at $\tau = 10$ (0.620 ROC area). Considering pairs of indicators do not improve much the performances: FLD resulting from the combination of ilv → sap interaction and dap entropy and at $\tau = 10$, both in paced breathing conditions, leads to a ROC area 0.671.

4. Discussion

In the present paper we have presented the MSE analysis of short term physiological time series. We have tested the robustness of our method for different lengths of the time series, and we have shown that the analysis of [15] can be successfully performed also on short rri recordings, still leading to separation between controls and patients. In the basal case, we have observed that controls have significantly higher entropy than CHF patients along wide scales intervals, and that dead patients show slightly less complex rri time series than the average over all patients. The severity of the pathology appears to be correlated with the loss of entropy. This picture is in agreement with findings in [15], corresponding to controls and subjects with congestive heart failure in sinus rhythm, except for a different form of the entropy curve for patients, which indeed depends on the pathology. Concerning the recalculation of the tolerance parameter r, we applied the prescription by Nikulin and Brismar [26], but similar results are obtained using the original prescription by [15]; in Figs. 10—13 we show the values of the entropy and of the probability that basal S_E values from controls and patients were drawn from the same distribution, evaluated by non-parametric test, versus τ; comparison with Figs. 4—7 reveals no significant differences in the curves and in the performance of the two methods. The usefulness of MSE as a tool in diagnosis and predictions has been tested with a ROC curve analysis, showing that, though performing quite fairly in

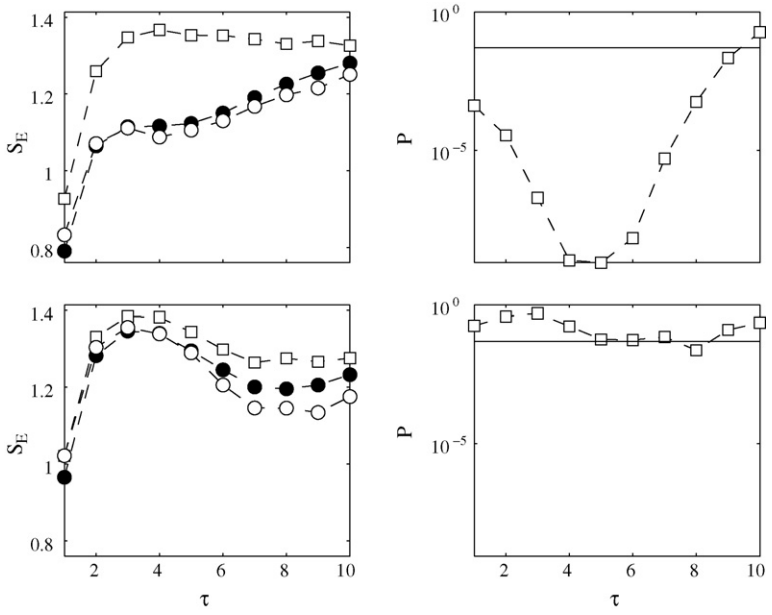

Figure 10 Sample entropy of rri time series plotted vs. τ, keeping the tolerance parameter r fixed as in [15]. Empty squares are the averages over the 47 healthy subjects, full circles are the averages over the 275 CHF patients, and empty circles are the averages over the 54 patients for whom cardiac death occurred. Top left: S_E in basal condition. Top right: the probability that basal S_E values from controls and patients were drawn from the same distribution, evaluated by non-parametric test. Bottom left: S_E in paced breathing condition. Bottom right: the probability that paced breathing S_E values from controls and patients were drawn from the same distribution, evaluated by non-parametric test.

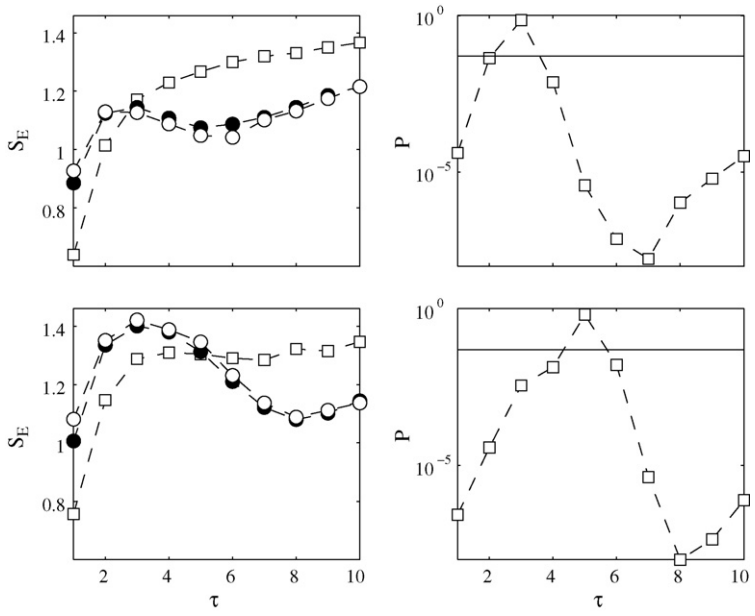

Figure 11 Sample entropy of sap time series plotted vs. τ, keeping the tolerance parameter r fixed as in [15]. Empty squares are the averages over the 47 healthy subjects, full circles are the averages over the 275 CHF patients, and empty circles are the averages over the 54 patients for whom cardiac death occurred. Top left: S_E in basal condition. Top right: the probability that basal S_E values from controls and patients were drawn from the same distribution, evaluated by non-parametric test. Bottom left: S_E in paced breathing condition. Bottom right: the probability that paced breathing S_E values from controls and patients were drawn from the same distribution, evaluated by non-parametric test.

separation, this analysis cannot be used as a diagnostic tool for single cases.

We extended the analysis by considering simultaneously acquired recordings of sap, dap and ilv. We have also proposed a multiscale approach to evaluate interactions between time series, by performing a multivariate AR modeling of the coarse grained time series. This analysis has put in evidence

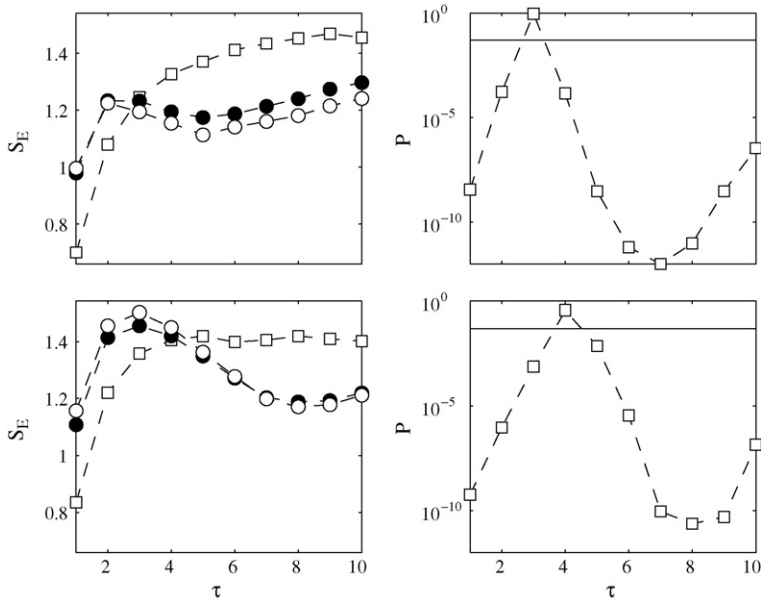

Figure 12 Sample entropy of dap time series plotted vs. τ, keeping the tolerance parameter r fixed as in [15]. Empty squares are the averages over the 47 healthy subjects, full circles are the averages over the 275 CHF patients, and empty circles are the averages over the 54 patients for whom cardiac death occurred. Top left: S_E in basal condition. Top right: the probability that basal S_E values from controls and patients were drawn from the same distribution, evaluated by non-parametric test. Bottom left: S_E in paced breathing condition. Bottom right: the probability that paced breathing S_E values from controls and patients were drawn from the same distribution, evaluated by non-parametric test.

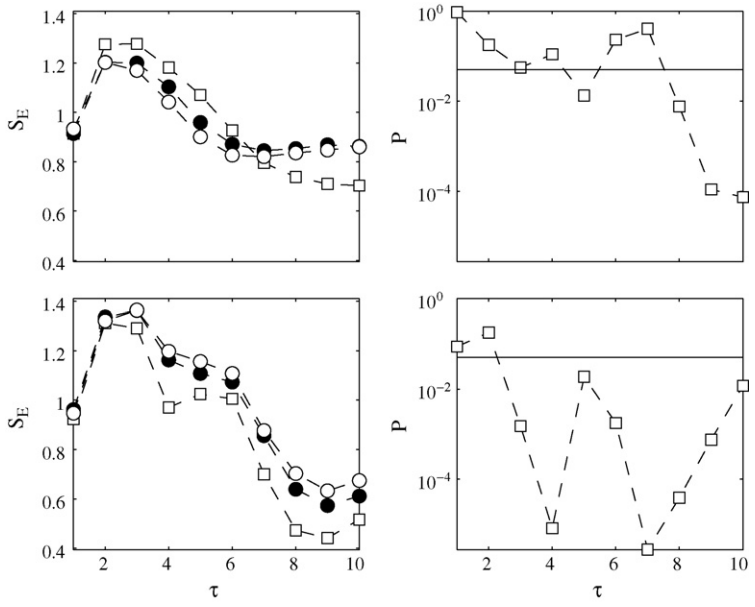

Figure 13 Sample entropy of ilv time series plotted vs. τ, keeping the tolerance parameter r fixed as in [15]. Empty squares are the averages over the 47 healthy subjects, full circles are the averages over the 275 CHF patients, and empty circles are the averages over the 54 patients for whom cardiac death occurred. Top left: S_E in basal condition. Top right: the probability that basal S_E values from controls and patients were drawn from the same distribution, evaluated by non-parametric test. Bottom left: S_E in paced breathing condition. Bottom right: the probability that paced breathing S_E values from controls and patients were drawn from the same distribution, evaluated by non-parametric test.

interesting patterns of interactions between time series, while providing several new quantitative indicators which are statistically correlated with the CHF pathology, and which can be employed for diagnosis of CHF patients.

Two mechanisms determine the feedforward influence rri → sap. Firstly the Starling law, stating that when the diastolic filling of the heart is increased or decreased with a given volume, the volume of blood which is then ejected from the heart increases or decreases by the same amount. More blood in: more blood out. This mechanism favors an increase of sap−dap as the rri interval increases, i.e. a positive coefficient rri → sap. The second mechanism is diastolic decay, described by the Windkessel model of the capacitative property of arteries; as rri interval increases, this effect tends to lower sap−dap values and gives a negative contribution to the coefficient rri → sap. Our finding suggests that the second mechanism is dominant. Evaluation of baroreflex regulation sap−dap → rri is an important clinical tool for diagnosis and prognosis in a variety of cardiac diseases [45]. Recent studies, see, e.g. [46] and references therein, have suggested that spontaneous fluctuations of arterial pressure and rri offer a noninvasive method for assessing baroreflex sensitivity without use of provocative tests employing injection of a vasoconstrictive drug or manipulation of carotid baroreceptor. It is worth stressing that the interaction dap → rri, evaluated by the present approach, has only little relation with the baroreflex sensitivity index considered, e.g. in [46]; indeed the procedures for evaluating these quantities differ in several steps. For example in our approach all time series are centered and normalized, hence the interaction between arterial pressure and rri is described only qualitatively.

Separating dead patients from alive patients is a very important task, since a good estimation of the probability of surviving of a given patient would be valuable when a decision has to be made with respect to the therapy to be undertaken. The separating performances provided by our indicators in this case are not good as those obtained separating patients and controls. Further work must be done to deal with the separation between dead patients and alive patients.

5. Conclusions

We have successfully extended the MSE analysis to short term time series coming from a cardiovascular care center. Furthermore we have shown that the multiscale approach is useful also when applied to multivariate AR modeling. Both types of analysis have indeed proved useful in separating patients

affected by CHF from control subjects. Our findings also suggest that the complexity-loss paradigm can be extended to the severity of the cardiac pathology.

References

[1] Akselrod S, Gordon D, Ubel FA, Shannon DC, Berger AC, Cohen RJ. Power spectrum analysis of heart rate fluctuation: a quantitative probe of beat-to-beat cardiovascular control. Science 1981;213(4504):220—2.

[2] Pinna GD, Maestri R, Raczak G, La Rovere MT. Measuring baroreflex sensitivity from the gain function between arterial pressure and heart period. Clin Sci (Lond) 2002;103(1): 81—8.

[3] Babloyantz A, Salazar JM, Nicolis G. Evidence of chaotic dynamics of brain activity during the sleep cycle. Phys Lett A 1985;111:152—6.

[4] Poon CS, Merrill CK. Decrease of cardiac chaos in congestive heart failure. Nature 1997;389:492.

[5] Ashkenazy Y, Ivanov PC, Havlin S, Peng CK, Goldberger AL, Stanley HE. Magnitude and sign correlations in heartbeat fluctuations. Phys Rev Lett 2001;86.

[6] Amaral LA, Goldberger AL, Ivanov PC, Stanley HE. Scale-independent measures and pathologic cardiac dynamics. Phys Rev Lett 1998;81:2388—91.

[7] Ivanov PC, Amaral LA, Goldberger AL, Havlin S, Rosenblum MG, Struzik ZR, et al. Multifractality in human heartbeat dynamics. Nature 1999;399(6735):461—5.

[8] Nunes Amaral LA, Ivanov PC, Aoyagi N, Hidaka I, Tomono S, Goldberger AL, et al. Behavioral-independent features of complex heartbeat dynamics. Phys Rev Lett 2001;86:6026.

[9] Lehnertz K, Elger CE. Can epileptic seizures be predicted? Evidence from nonlinear time series analysis of brain electrical activity. Phys Rev Lett 1998;80:5019—22.

[10] Peng CK, Mietus J, Hausdorff JM, Havlin S, Stanley HE, Goldberger AL. Long-range anticorrelations and non-Gaussian behavior of the heartbeat. Phys Rev Lett 1993;70:1343—6.

[11] Ivanov PC, Nunes Amaral LA, Goldberger AL, Havlin S, Rosenblum MG, Stanley HE, et al. From $1/f$ noise to multifractal cascades in heartbeat dynamics. Chaos 2001;11:641—52.

[12] Tass P, Rosenblum MG, Weule J, Kurths J, Pikovsky A, Volkmann J, et al. Detection of n:m phase locking from noisy data: application to magnetoencephalography. Phys Rev Lett 1998;81(15):3291—4.

[13] Franaszczuk PJ, Blinowska KJ, Kowalczyc M. The application of parametric multichannel spectral estimates in the study of brain activity. Biol Cybern 1985;(51):239—47.

[14] Korzeniewska A, Manczak M, Kaminski M, Blinowska KJ, Kasicki S. Determination of information flow direction among brain structures by a modified directed transfer function (dDTF) method. J Neurosci Methods 2003;125(1—2):195—207.

[15] Costa M, Goldberger AL, Peng CK. Multiscale entropy analysis of complex physiologic time series. Phys Rev Lett 2002;89(6):068102.

[16] Ferrario M, Signorini MG, Magenes G, Cerutti S. Comparison of entropy-based regularity estimators: application to the fetal heart rate signal for the identification of fetal distress. IEEE Trans Biomed Eng 2006;53(1):119—25 [Controlled clinical trial].

[17] Costa M, Peng CK, Goldberger AL, Hausdorff JM. Multiscale entropy analysis of human gait dynamics. Phys A: Stat Mech Appl 2003;330:53—60.

[18] Bhattacharya J, Edwards J, Mamelak AN, Schuman EM. Long-range temporal correlations in the spontaneous spiking of neurons in the hippocampal-amygdala complex of humans. Neuroscience 2005;131(2):547—55.

[19] Lee UC, Kim S, Yi SH. Event and time-scale characteristics of heart-rate dynamics. Phys Rev E 2005;71(6):061917.

[20] Wessel N, Schirdewan A, Kurths J. Intermittently decreased beat-to-beat variability in congestive heart failure. Phys Rev Lett 2003;91(11):119801.

[21] Thuraisingham RA, Gottwald GA. On multiscale entropy analysis for physiological data. Physica A 2006;366: 323—32.

[22] Govindan RB, Wilson JD, Eswaran H, Lowery CL, Preissl H. Revisiting sample entropy analysis. Physica A 2007;376: 158—64.

[23] Pincus SM. Approximate entropy as a measure of system complexity. Proc Natl Acad Sci USA 1991;88:2297—301.

[24] Richman JS, Moorman JR. Physiological time-series analysis using approximate entropy and sample entropy. Am J Physiol Heart Circ Physiol 2000;278(6):2039—49.

[25] Goldberger AL, Peng CK, Lipsitz LA. What is physiologic complexity and how does it change with aging and disease? Neurobiol Aging 2002;23(1):23—6 [Comment].

[26] Nikulin VV, Brismar T. Comment on ''Multiscale entropy analysis of complex physiologic time series''. Phys Rev Lett 2004;92(8):089803 [author reply 089804, February 2004, Comment].

[27] Costa M, Goldberger AL, Peng CK. Costa, Goldberger, and Peng reply. Phys Rev Lett 2004;92(8):089804.

[28] Costa M, Goldberger AL, Peng CK. Multiscale entropy analysis of biological systems. Phys Rev E 2005;71:21906—23.

[29] Kantz H, Schreiber T. Nonlinear time series analysis. Cambridge, UK: Cambridge University Press; 1997.

[30] Schreiber T. Measuring information transfer. Phys Rev Lett 2000;85:461—4.

[31] Cooke WH, Cox JF, Diedrich AM, Taylor JA, Beightol LA, Ames JE, et al. Controlled breathing protocols probe human autonomic cardiovascular rhythms. Am J Physiol 1998;274(2 Pt 2):709—18.

[32] Rzeczinski S, Janson NB, Balanov AG, McClintock PV. Regions of cardiorespiratory synchronization in humans under paced respiration. Phys Rev E 2002;66(5):051909.

[33] Pinna GD, Maestri R, La Rovere MT, Gobbi E, Fanfulla F. Effect of paced breathing on ventilatory and cardiovascular variability parameters during short-term investigations of autonomic function. Am J Physiol Heart Circ Physiol 2006;290(1): H424—33.

[34] Maestri R, Pinna GD. Polyan: a computer program for polyparametric analysis of cardiorespiratory variability signals. Comput Methods Programs Biomed 1998;56(1):37—48.

[35] Ancona N, Maestri R, Marinazzo D, Nitti L, Pellicoro M, Pinna GD, et al. Leave-one-out prediction error of systolic arterial pressure time series under paced breathing. Physiol Meas 2005;26(4):363—72 [Clinical trial].

[36] Mann HB, Whitney DR. On a test of whether one of 2 random variables is stochastically larger than the other. Ann Math Stat 1947;(18):50—60.

[37] Schafer C, Rosenblum MG, Kurths J, Abel HH. Heartbeat synchronized with ventilation. Nature 1998;392(6673):239—40 [Letter].

[38] Lake DE, Richman JS, Griffin MP, Moorman JR. Sample entropy analysis of neonatal heart rate variability. Am J Physiol Regul Integr Comp Physiol 2002;283(3):789—97.

[39] Swets JA. Measuring the accuracy of diagnostic systems. Science 1988;240:1285.

[40] Miyakawa K, Polosa C, Koepchen HP. Mechanisms of blood pressure waves. Berlin: Springer; 1984.

[41] Hirsch JA, Bishop B. Respiratory sinus arrhythmia in humans: how breathing pattern modulates heart rate. Am J Physiol 1981;241(4):620—9.
[42] Schafer C, Rosenblum MG, Abel HH, Kurths J. Synchronization in the human cardiorespiratory system. Phys Rev E 1999;60(1):857—70.
[43] Angelini L, Lattanzi G, Maestri R, Marinazzo D, Nardulli G, Nitti L, et al. Phase shifts of synchronized oscillators and the systolic—diastolic blood pressure relation. Phys Rev E 2004;69:061923—9128.
[44] deBoer RW, Karemaker JM, Strackee J. Hemodynamic fluctuations and baroreflex sensitivity in humans: a beat-to-beat model. Am J Physiol Heart Circ Physiol 1987;253(3):H680—9.
[45] Pinna GD, Maestri R, Capomolla S, Febo O, Robbi E, Cobelli F, et al. Applicability and clinical relevance of the transfer function method in the assessment of baroreflex sensitivity in heart failure patients. J Am Coll Cardiol 2005;46(7):1314—21.
[46] Nollo G, Faes L, Porta A, Antolini R, Ravelli F. Exploring directionality in spontaneous heart period and systolic pressure variability interactions in humans: implications in the evaluation of baroreflex gain. Am J Physiol Heart Circ Physiol 2005;288(4):1777—85.